



Article

Chopped Basalt Fiber-Reinforced High-Performance Concrete: An Experimental and Analytical Study

Ahmed M. Tahwia , Khaled A. Helal and Osama Youssf * 

Structural Engineering Department, Faculty of Engineering, Mansoura University, Mansoura 35516, Egypt; atahwia@mans.edu.eg (A.M.T.); khaledahmed8200@gmail.com (K.A.H.)

* Correspondence: osama.youssf@mymail.unisa.edu.au

Abstract: Basalt fiber (BF) is an environmentally friendly type of fiber that has attracted the attention of researchers in recent years due to its excellent performance in concrete constructions. This current research was conducted to investigate the effect of chopped basalt fiber on the workability, compressive strength, and impact resistance of high-performance concrete (HPC). Three various lengths (3, 12, and 18 mm) and six volume fractions (0%, 0.075%, 0.15%, 0.3%, 0.45%, and 0.6% by concrete volume) of BF were used in producing sixteen HPC mixes. HPC compressive strength and impact resistance were measured for each mix. Scanning electron microscopy (SEM) analysis was also conducted on selected mixes to closely investigate the effects of the applied variables through the microstructural scale. An empirical model was developed to study the relationship between the impact energy and compressive strength of BF-reinforced HPC. The results show that adding BF improves the compressive strength and impact resistance. Compared with the control concrete, the compressive strength of the HPC reinforced with 3 mm, 12 mm, and 18 mm BF increased by 12.2%, 15.1%, and 17.5%, respectively. The impact resistance increased with a dosage of 8 kg/m³ for all lengths of BF. The SEM observations revealed that the BF accumulated in pores and on the surface of the attached cement which improved the microstructure of the interfacial transition zone (ITZ), which further enhanced the strength and ductility of the HPC.

Keywords: high-performance concrete; basalt fibers; compressive strength; impact resistance; SEM analysis



Citation: Tahwia, A.M.; Helal, K.A.; Youssf, O. Chopped Basalt Fiber-Reinforced High-Performance Concrete: An Experimental and Analytical Study. *J. Compos. Sci.* **2023**, *7*, 250. <https://doi.org/10.3390/jcs7060250>

Academic Editor: Francesco Tornabene

Received: 11 May 2023

Revised: 7 June 2023

Accepted: 12 June 2023

Published: 15 June 2023



Copyright: © 2023 by the authors. Licensee MDPI, Basel, Switzerland. This article is an open access article distributed under the terms and conditions of the Creative Commons Attribution (CC BY) license (<https://creativecommons.org/licenses/by/4.0/>).

1. Introduction

Concrete is widely used in almost all civil engineering fields such as roads, bridges, and buildings because of its abundant raw materials, ease of construction, and high compressive strength [1]. However, the low tensile strength and large shrinkage and deformation of plain concrete (PC) limit its further development [2]. In order to solve this difficulty and improve the use of concrete characteristics, scholars have found that the addition of fibers can improve the performance of concrete, making it a new composite material [3]. PC is considered to be a crackable material under tensile stresses due to its relatively low tensile strength. Using randomly distributed fibers in concrete can control the development of concrete cracks, and this concrete type is known as fiber-reinforced concrete (FRC) [4].

Fiber-reinforced concrete (FRC) is extensively used in engineering structures due to its favorable mechanical properties and durability, especially for structures under harsh environments, such as hydraulic and coastal structures [5]. A variety of fibers were used in previous studies, including steel fiber [6,7], glass fiber [8], carbon fiber [9], and organic fibers such as polyethylene terephthalate fiber. Those fibers nevertheless held a series of drawbacks such as high density, high using cost, low resistance to chemical corrosion, and so forth [10]. Fiber-reinforced polymer (FRP) has been used in the construction industry due to its ability to increase energy absorption, as well as its corrosion resistance, tensile stiffness, and strength [11,12]. FRP is anticipated to provide structures with substantial energy absorption ability and deformability when subjected to extreme conditions such as

impact loads and seismic actions. In practice, encapsulating concrete elements using glass or carbon FRP provides a superior substitution to reinforced concrete structures that are periodically subjected to dynamic loads such as the following: marine fender piers, piles and girders of bridges, and road barriers [13,14].

Basalt fiber [15,16], an inorganic fiber extracted from melted volcanic basalt rock, is currently available commercially. The reasons for this are comprehensively summarized as follows: (a) less energy consumption and no chemical additive during the production process coupled with the widespread availability of raw materials, which all make the basalt fiber more eco-friendly and cheaper than some other fibers; (b) excellent dispersion ability in the mixing, and thus there is not a need to mix in additional dispersion agents or plasticizers, due to the addition of the basalt fiber; and (c) other advantages such as that basalt fiber is non-toxic, has good resistance to chemical attacks, has heat resistance, has superior interfacial bond strength with cement materials, etc., even though the mechanical properties of a single fiber are relatively not as prominent as those of carbon fiber or others. The dimensions of the fiber vary in a significant range, from 10 to 20 μm in diameter and from 3 to 130 mm in length [15].

Therefore, the application of short chopped basalt fibers (CBFs) with a length in the range from about 3 to 24 mm [17], is becoming popular in recent years. Alaskar et al. [18] suggested that using shorter fibers distributed in concrete is a more effective method to avoid micro-cracks and progressive spalling. In [19], CBFs of 3, 6, 12, and 24 mm in length were mixed with a fiber volume up to 0.5%, and the results showed that the highest flexural and splitting tensile strengths are obtained in the concrete with fiber volume and length of 0.5% and 24 mm, respectively, while the highest compressive strength corresponds to the volume and length of 0.1% and 12 mm, respectively. Sadrmomtazi et al. [16] pointed out that high amounts of fibers (more than 1.0%) cause severe mixing and casting problems, in spite of great improvement in basic strengths. Niu et al. [20] indicated that adding 18 mm CBFs at 0.1–0.2% volume presents superior mechanical properties together with the best chloride resistance. Jiang et al. [21] conducted a comprehensive analysis including workability, strength, toughness, and durability, deducing that the optimum volume is 0.1% for CBFs with 12 mm, while in the meanwhile, its workability is compromised but still meets specification. Adesina et al. [22] reviewed extensive influence factors, and recommended that preliminary trials should be carried out to find the optimum volume and length for a specified application of FRC before its application on a structural scale, such as flexural members.

Some previous studies explored the performance of BF in concrete and showed variable effects on its mechanical properties. Jiang et al. [21] showed that adding 1% BF increased the concrete's compressive and flexural strengths and decreased the drying shrinkage in early ages. El-Shafie and Whittleston [23] carried out an experimental study on the use of different chopped BF lengths and contents on the compressive strength of normal concrete. The study reported some strength enhancements when 12 mm and 24 mm chopped BF with contents between 0.1% and 0.5% were used. Similarly, Wang et al. [24] used BF as reinforcement for high-performance concrete. Results from the study indicated that the compressive strength of the concrete mixtures increased when using up to 0.2% dosage of BF. Concrete mixtures reinforced with 12 mm and 22 mm BF at a dosage of 0.1% were 4.6% and 5.7% higher in compressive strength than that of the concrete without BF. Irine [25] used chopped BF using three different contents (1, 2, and 4 kg/m^3) and the results showed that increasing the BF content increased the compressive strength, splitting tensile strength, and flexural strength by 14%, 62%, and 54%, respectively, compared with no use of BF. Another researcher investigated the effect of BF dosage and length on the slump of concrete mixtures. Results from the study showed that the slump of concrete mixtures decreased with the increasing length and dosage of BF. The slump of mixtures reinforced with 12 mm BF at a dosage of 0.05%, 0.1%, 0.3%, and 0.5% was 7%, 15%, 53%, and 65% lower than the concrete mixtures with no BF, respectively, compared with reference concrete [21].

Some previous studies have shown a variety of effects of the addition of BF on compressive strength at a certain number of days. A study reported that the addition of BF at 1.0% volume fraction caused an increase of 8.92% on the compressive strength within 28 days [26]. Another study reported that the BFRC's compressive strength was 4.22% higher than that of plain concrete at a fiber content of 0.3% volume fraction [1]. According to Jiang et al. [21], the addition of BF at 0.1% volume fraction caused an increase of 5.72% on the BFRC compressive strength within 28 days. The design of concrete buildings depends mainly upon the concrete strength and serviceability with less concentration on its durability and resistance to environmental effects. More attention should be paid to durability-based approaches in all stages of building. Such stages included designation, execution, operation, and maintenance.

High-performance concrete (HPC) is a type of concrete that is characterized by its high strength, high workability, and high durability [27]. The American Concrete Institute committee defined HPC as the concrete that provides special performance and uniformity which could not be accomplished by traditional concrete. The compressive strength of HPC was considered to be about 55–150 MPa. Using HPC in the construction industry saves significant time required for constructing, as well as transportation costs. HPC has the features of easy molding, high workability, high strength gains in early ages, high mechanical properties in late ages, high modulus of elasticity, high toughness, high abrasion resistance, lower permeability, high resistance to chemical attack, and low volume stability [28]. The addition of a single fiber can only improve the performance of a single aspect of the concrete. Enhancing the overall performance of concrete can be achieved by mixing it with different fibers [29]. BF could significantly improve the deformation and energy absorption capacities of concrete [30]. In comparison to fibers such as glass and carbon fibers, BF is rarely used for large-scale applications due to the limited research and understanding of its performance in concrete.

Therefore, the aim of the current study is to evaluate the effects of the volume fraction and the length of chopped BF and the replacement ratio on the physical and mechanical properties of HPC and BF together. In addition, a microstructure analysis was conducted to provide insight into understanding the microstructures of HPC and BF in relation to their mechanical properties. This research would help to understand the mechanical properties of HPC and broaden the applications of BF in structural engineering applications.

2. Experimental Program

2.1. Materials

All concrete mixes were made with type CEM I 52.5 Portland cement produced by “Al-Arish” company and conforming to the Egyptian standard ES 4756-1/2013 [31]. Crushed dolomite of 10 mm derived from locally available quarry “Attaqa” and conforming to the ES 1109/2008 [32] was used as coarse aggregate. Natural local sand having a fineness modulus of 2.95 was utilized as fine aggregate. Locally obtainable silica fume (SF) supplied by Egyptian Ferro Alloys Corporation was used as additional cementitious material in all mixes. Three different lengths of chopped BF, namely, 3 mm, 12 mm, and 18 mm with six volume fractions (0%, 0.075%, 0.15%, 0.3%, 0.45%, and 0.6% by concrete volume), were used to produce the HPC. The configurations of BF used in this experimental work is illustrated in Figure 1 and their characteristics are presented in Table 1. To achieve the desired workability, a commercially high-performance polycarboxylate superplasticizer (Sika Visco-Crete-5930) was used in the mixes. This superplasticizer (SP) type is specifically designed to produce HPC and meets the requirements of ASTM C494 Type G and F [33].

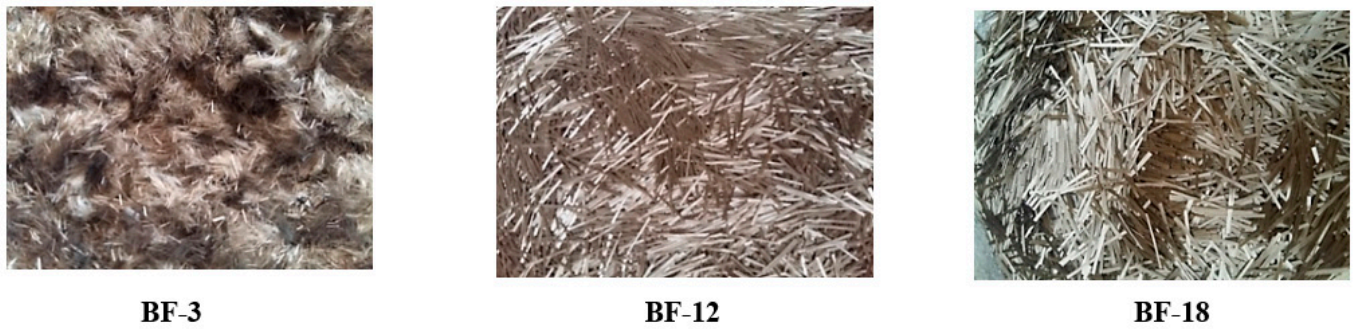


Figure 1. Configuration of basalt fibers used in this study.

Table 1. Basalt fiber characteristics.

Property	Cut Length (mm)	Diameter (μm)	Density (gm/cm^3)	Elastic Modulus (GPa)	Elongation at Break (%)	Tensile Strength (MPa)
BF-3	3	13	2.65	83	3.1	2574
BF-12	12	15	2.65	62	2.9	2450
BF-18	18	15	2.65	62	2.9	2450

2.2. Concrete Mix Design

Table 2 gives the details of the proportions of concrete mixes in this study. Sixteen HPC mixes were designed with constant cement content of 450 kg/m^3 , SF content of 50 kg/m^3 (10% of the binder), sand content of 625 kg/m^3 , dolomite content of 1075 kg/m^3 , water content of 150 kg/m^3 (water/binder of 0.3), and SP content of 10 kg/m^3 . BF with different lengths, including 3 mm, 12 mm, and 18 mm, and different contents, including 2, 4, 8, 12, and 16 kg/m^3 , have been implemented. The mix denotation is labeled according to fiber length and content. For example, mix BF-18-8 indicates that basalt fibers of 18 mm length were used at a content of 8 kg/m^3 .

Table 2. Mix proportions of concrete mixes.

Mix Code	Fiber Length (mm)	V_f (%)	Cement (kg/m^3)	Silica Fume (kg/m^3)	Sand (kg/m^3)	Dolomite (kg/m^3)	Water (kg/m^3)	SP (kg/m^3)	BF (kg/m^3)
BF-0	-	0	450	50	625	1075	150	10	-
BF-3-2	3	0.075	450	50	625	1075	150	10	2
BF-3-4	3	0.15	450	50	625	1075	150	10	4
BF-3-8	3	0.3	450	50	625	1075	150	10	8
BF-3-12	3	0.45	450	50	625	1075	150	10	12
BF-3-16	3	0.6	450	50	625	1075	150	10	16
BF-12-2	12	0.075	450	50	625	1075	150	10	2
BF-12-4	12	0.15	450	50	625	1075	150	10	4
BF-12-8	12	0.3	450	50	625	1075	150	10	8
BF-12-12	12	0.45	450	50	625	1075	150	10	12
BF-12-16	12	0.6	450	50	625	1075	150	10	16
BF-18-2	18	0.075	450	50	625	1075	150	10	2
BF-18-4	18	0.15	450	50	625	1075	150	10	4
BF-18-8	18	0.3	450	50	625	1075	150	10	8
BF-18-12	18	0.45	450	50	625	1075	150	10	12
BF-18-16	18	0.6	450	50	625	1075	150	10	16

2.3. Mixing Procedure and Specimens Preparation

All concrete ingredients, except the fibers, were firstly mixed dry for 2 min in a pan mixer, then half of the mixing water and all superplasticizer were added and mixed for another 3 min. The remaining half of the water and BF were then added and mixed for 3 min.

Three concrete cubes of 100 mm size and one cylinder of 150 × 300 mm per testing day were cast from each mix for measuring the compressive strength and impact resistance, respectively. The specimens were mechanically compacted using a vibrating table and left for 24 h before demolding and curing in water at 20 °C until the testing day. The compressive strength was measured according to the Egyptian Standard [34] at 2, 28, and 56 days. Four concrete discs with 150 mm diameter and 65 mm thickness were cut from the 150 × 300 mm cylinders at 28 days concrete age using a concrete saw to test the concrete impact resistance through a drop-weight test according to ACI committee 544 guidelines [35].

3. Results and Discussion

3.1. Workability

The effects of BF length and dosage on the HPC slump are presented in Table 3 and Figure 2. It can be seen that all mixes incorporating BF had a lower slump compared to the plain concrete mix (BF-0), as shown in Figure 3. With increasing the BF content or the BF length, the slump decreased. Using 0.075%, 0.15%, 0.30%, 0.45%, and 0.6% dosages of BF in HPC decreased its slump by 18%, 32%, 50%, 64%, and 77%, respectively, for the 3 mm BF; by 29%, 39%, 63%, 68%, and 84%, respectively, for the 12 mm BF; and by 38%, 57%, 71%, 82%, and 93%, respectively, for the 18 mm BF. Increasing the BF length at 3 mm, 12 mm, and 18 mm decreased the HPC slump by 18%, 29%, and 38%, respectively, at BF volume of 0.075%; by 32%, 39%, and 57%, respectively, at BF volume of 0.15%; by 50%, 63%, and 71%, respectively, at BF volume of 0.30%; by 64%, 68%, and 82%, respectively, at BF volume of 0.45%; and by 77%, 84%, and 93%, respectively, at BF volume of 0.6%. The slump decrease with BF dosage increase is attributed to the high water absorption of the BF which results in a decrease in the free water content within the concrete matrix. In addition, the relatively large surface area of the BF results in a decrease in the available cementitious material needed for lubrication within the concrete matrix, and hence the concrete slump decreases. Sadrumontazi et al. (2018) [16] mentioned that there was a huge balling effect in mortar mixes reinforced with a high dosage of BF which negatively affected the mortars' mixing and placing.

Table 3. HPC slump test results.

Mixture (ID)	Fiber Dosage (kg/m ³)	Slump (mm)
BF-0	-	280
BF-3-2	2	230
BF-3-4	4	190
BF-3-8	8	140
BF-3-12	12	100
BF-3-16	16	65
BF-12-2	2	200
BF-12-4	4	170
BF-12-8	8	105
BF-12-12	12	90
BF-12-16	16	45
BF-18-2	2	175
BF-18-4	4	120
BF-18-8	8	80
BF-18-12	12	50
BF-18-16	16	20

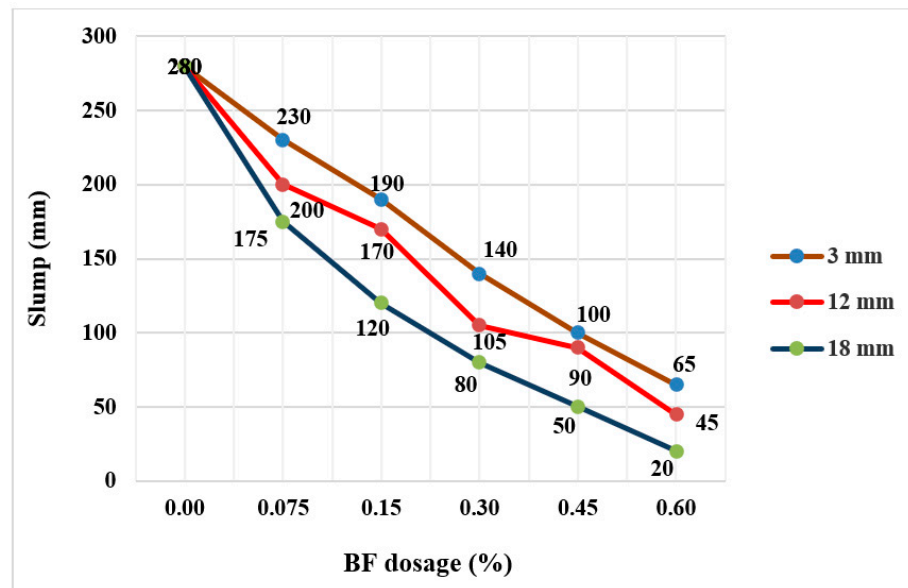


Figure 2. Effect of BF content and dosage on HPC slump.



Figure 3. Slump measure during casting.

The observed adverse effect on HPC slump with increasing the BF length is attributed to the increase in the existent fibers per unit volume. In addition, distributing the fibers within the concrete matrix becomes more difficult when using lengthy fiber size that causes non-uniformity among the concrete ingredients, and hence a slump reduction.

3.2. Compressive Strength

Different conclusions have been drawn on the effect of BF on the compressive strength of concrete. Wang et al. [24] indicated that concrete samples reinforced with CBFs of 12 mm and 22 mm at a volume of 0.10% were around 5% higher than that of normal concrete. The test results obtained from Jiang et al. [21] were that the strength-effectiveness at 7 days was higher than that at 28 days, and almost no fluctuation was observed for strengthened samples in the program when compared to normal concrete at 28 days. This is possibly because there was an obvious increase in the total pore volume and porosity at 7 and 28 days, which was adverse to the improvement of mechanical behavior. Among several comparisons of strengths, most of the studies show that the optimum volume seems to be the volume fraction, although the compressive strength is still under debate and hardly provides a clear explanation [30].

Table 4 displays the measured average compressive strength of the tested sixteen HPC mixes at 2, 28, and 56 days concrete age. Figures 4–6 show the variation in HPC compressive strength at all concrete ages. Compared with no BF in mix BF-0, increasing the fiber content increased the HPC compressive strength at 2 days by up to 12%, 14.1%, and 16%, respectively; at 28 days by up to 12.2%, 15.1%, and 17.5%, respectively; and at 56 days by up to 7.9%, 12.8%, and 9.5%, respectively, when using 3 mm, 12 mm, and 18 mm BF lengths. These peak strength enhancements were achieved when BF was used with a volume fraction of 0.3% in mixes BF-3-8, BF-12-8, and BF-18-8. However, beyond 0.3% BF, the compressive strength started to decrease with increasing the BF content. The possible reduction in the compressive strength at higher dosages could be a result of the formation of voids inside the composite which yielded a poor interfacial zone between the BF and the cementitious matrix. Therefore, adding a proper amount of fiber can improve the strength and toughness of HPC, but if the fiber fraction is too high, the internal defects increase, which is not conducive to the improvement of strength [19]. Moreover, with the increased dosage of fiber, it is more difficult for the fiber to uniformly distribute within the cementitious composites, which adversely affects the strength development.

The highest compressive strength enhancements were observed at a concrete age of 28 days compared with those at 2 or 56 days, as shown in Table 4. This was due to the fact that the compressive strength increase for the HPC at 28 days was higher than that at the early age (2 days). In addition, there was even a decrease in the compressive strength of BF concrete at 56 days. This might be attributed to the poor interface adhesion between the fibers and the concrete matrix that led to a drop in the substrate’s bonding capacity [21,22]. Moreover, it can be found from the above results that the length of basalt fiber has a beneficial effect on compressive strength, but it is not very obvious. The use of 18 mm BF in concrete shows a larger increase in compressive strength than that of 12 mm or 3 mm BF. The reason may be that the longer fiber has a stronger bridging effect and pulling-out resistance, which contribute to the strength development.

Table 4. Results of compressive strength for all mixes.

Mix Code	Fiber Length (mm)	V _f (%)	Compressive Strength (MPa)					
			2 Days		28 Days		56 Days	
			Measured (MPa)	Strength Enhancement (%)	Measured (MPa)	Strength Enhancement (%)	Measured (MPa)	Strength Enhancement (%)
BF-0	-	0	46.8	-	86.3	-	99.6	-
BF-3-2	3	0.075	47	0.4	86.8	0.6	99.3	-0.3
BF-3-4	3	0.15	48.6	3.8	88.4	2.4	101.7	2.1
BF-3-8	3	0.3	52.4	12.0	96.8	12.2	107.5	7.9
BF-3-12	3	0.45	49.3	5.3	91.2	5.7	102.5	2.9
BF-3-16	3	0.6	48.1	2.8	89.8	4.1	99.8	0.2
BF-12-2	12	0.075	47.9	2.4	89	3.1	101.3	1.7
BF-12-4	12	0.15	49.7	6.2	92.7	7.4	105.1	5.5
BF-12-8	12	0.3	53.4	14.1	99.3	15.1	112.3	12.8
BF-12-12	12	0.45	51.2	9.4	93.7	8.6	103.6	4.0
BF-12-16	12	0.6	49.1	4.9	91.2	5.7	101.2	1.6
BF-18-2	18	0.075	49.4	5.6	90.5	4.9	102.3	2.7
BF-18-4	18	0.15	51.2	9.4	95.3	10.4	107.8	8.2
BF-18-8	18	0.3	54.3	16.0	101.4	17.5	114	14.5
BF-18-12	18	0.45	52.5	12.2	96.3	11.6	105.7	6.1
BF-18-16	18	0.6	50.8	8.6	93.8	8.7	102.7	3.1

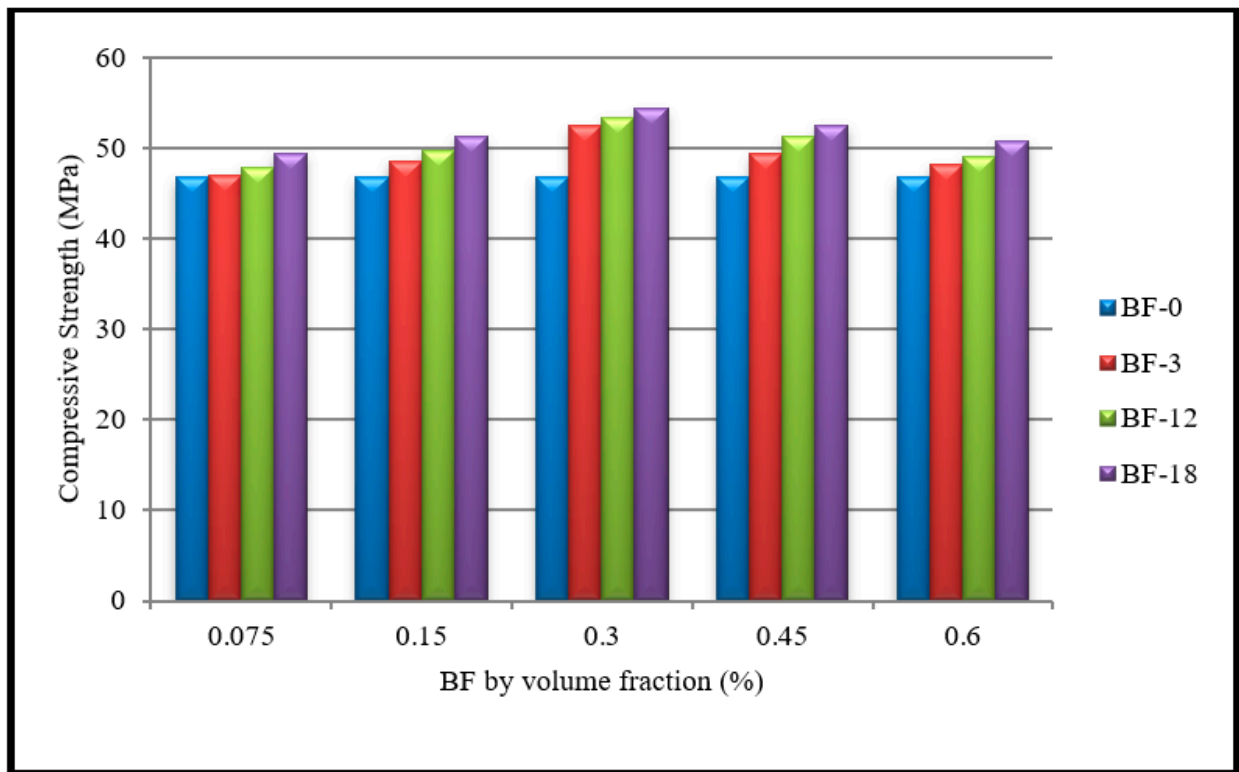


Figure 4. Variation in compressive strength at 2 days.

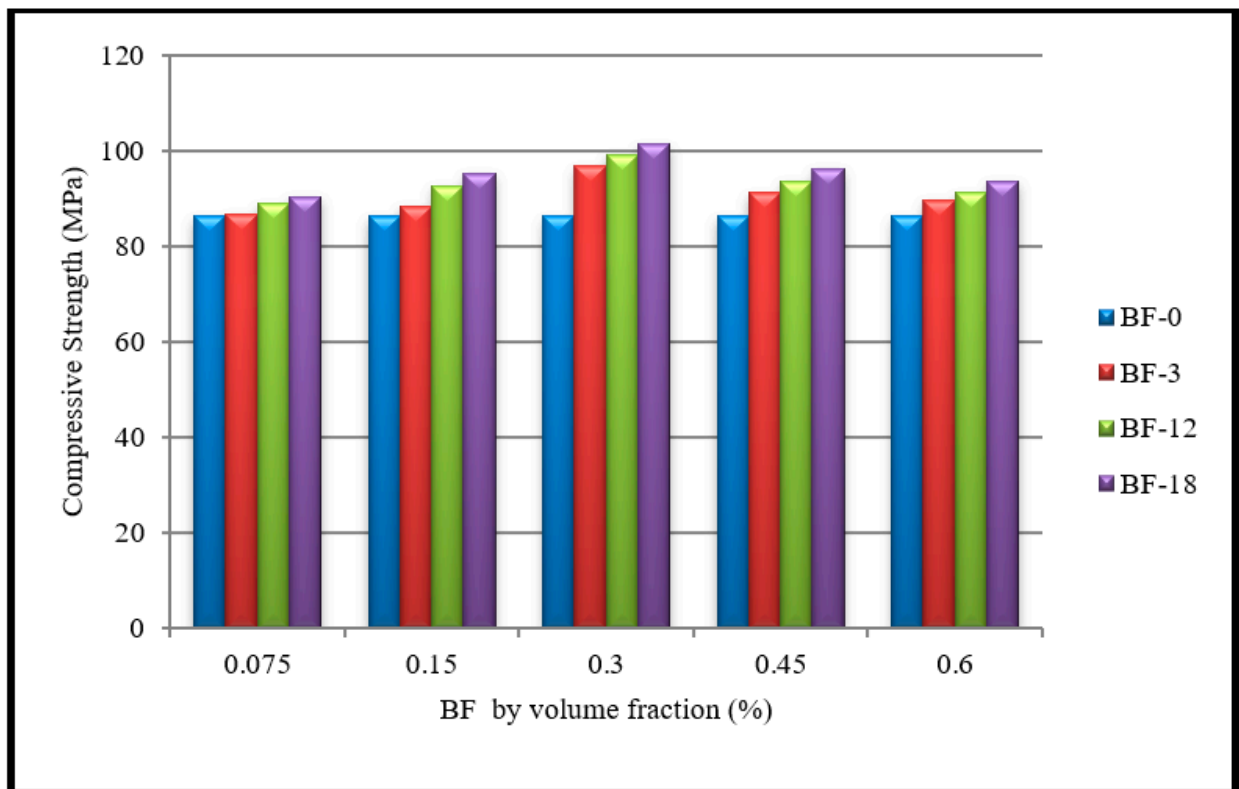


Figure 5. Variation in compressive strength at 28 days.

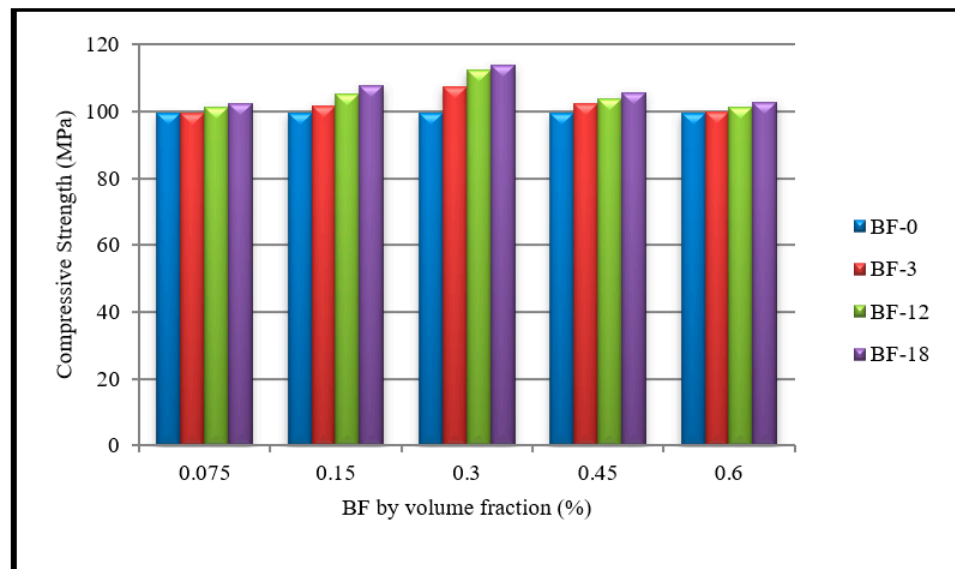


Figure 6. Variation in compressive strength at 56 days.

3.3. Impact Resistance

Drop-weight tests were used to measure the impact resistance of HPC mixes in this study. The test method is a modified version of that of the American Concrete Institute (ACI) committee, as recommended by Badr and Ashour [36]. The process is attained through a steel hammer with a total mass of 13.5 kg dropping from a 457 mm height onto a steel ball with a 63.5 mm diameter which is placed upon the central surface of the cylindrical (150 × 65 mm) concrete disc specimens made with a 25.4 mm triangular notch. Figures 7 and 8 show the drop-weight test setup. The number of blows required to cause a visible surface crack and subsequent failure were recorded for each specimen. Failure was defined by either complete separation of the specimen or the impact piston being fully embedded in the concrete [4].



Figure 7. Impact test rig.



Figure 8. Concrete disc specimen.

In compliance with the ACI 544 committee report, the number of blows which are required to produce the crack initiation have been recorded as the total strength of such an initial crack; however, the number of blows which are required to obtain the complete failure of the specimen are recorded as the strength of the fracture. Such a technical method is used by various previous researchers [37,38]. The capacity of energy absorption used within the test has been calculated through the use of Equation (1) [39]:

$$IE = mgHN \quad (1)$$

where

- IE —impact energy (N.m),
- m —the mass of dropped ball (13.5 Kg),
- g —the gravity-based acceleration (9.8 m/s²),
- H —the height of drop (457 mm),
- N —number of blows at ultimate failure.

These values are similar to those reported by other researchers using the same test method [36,40]. This high variation in behavior could deter the practical application of the fiber, since it is probable that a practicing engineer would prefer to have a higher level of certainty in expected behavior [4]. Additionally, the results are confined to the loading conditions of the test method (13.5 kg dropped from 457 mm).

In terms of the influence of BF on impact, the results from the study by Branston et al. [4] indicated that BF had no significant effect on the impact resistance of concrete. However, the study by Niaki et al. [29] on polymer concrete showed that the incorporation of BF resulted in the higher impact resistance of the polymer concrete up to a dosage of 3%. Moreover, the reduction at higher BF dosage in the study by Niaki et al. [29] can also be attributed to the balling effect which results in less activation of the fibers as they are clumped together.

Table 5 illustrates the drop-weight impact test results. In this table, V_f is the volume fraction of basalt fibers, t is the thickness of the specimen, and D is the diameter of the specimen. Figure 9 demonstrates the average impact toughness (Energy/volume) of the HPC mixes, compared to the control mix (BF-0). It is clear from the figure that the addition of BF to the HPC has a direct effect on the impact toughness. At any BF length, increasing

the fiber content up to 0.3% increased the impact toughness. Beyond that, the impact toughness showed relatively less increase or decrease compared with the corresponding control mix BF-0. Using 0.075%, 0.15%, 0.3%, and 0.45% fiber contents increased the impact toughness by 3%, 33%, 101%, and 73%, respectively, at 3 mm length BF; by 24%, 97%, 194%, and 149%, respectively, at 12 mm length BF; and by 86%, 261%, 361%, and 298%, respectively, at 18 mm length BF. The increase in impact toughness with increasing the BF content is attributed to the crack-bridging effect that delayed the cracks' initiation and limited the cracks' propagation.

Table 5. Test results for impact energy and impact toughness.

Mixture No.	Fiber Length (mm)	V_f (%)	Number of Drop	t (mm)	D (mm)	Specimen Volume (m^3)	Impact Energy (J)	Specimen Mass (kg)	Energy/Volume (kJ/m^3)	Energy/Mass (J/kg)
BF-0	-	0	22	65	151	1.163×10^{-3}	1331.5	2.65	1144.9	502.4
BF-3-2	3	0.075	23	66	151	1.181×10^{-3}	1392.0	2.78	1178.6	500.7
BF-3-4	3	0.15	28	63	150	1.112×10^{-3}	1694.6	2.68	1523.9	632.3
BF-3-8	3	0.3	43	64	150	1.130×10^{-3}	2602.4	2.71	2303	960.3
BF-3-12	3	0.45	36	63	149	1.098×10^{-3}	2178.8	2.61	1984.3	834.8
BF-3-16	3	0.6	18	64	149	1.115×10^{-3}	1089.4	2.63	977.0	414.2
BF-12-2	12	0.075	27	65	150	1.148×10^{-3}	1634.0	2.69	1423.3	607.4
BF-12-4	12	0.15	41	64	148	1.100×10^{-3}	2481.4	2.61	2255.8	950.7
BF-12-8	12	0.3	64	66	149	1.150×10^{-3}	3873.4	2.73	3368.2	1418.8
BF-12-12	12	0.45	54	65	150	1.148×10^{-3}	3268.2	2.71	2846.9	1206.0
BF-12-16	12	0.6	19	66	150	1.165×10^{-3}	1150.0	2.68	987.1	429.1
BF-18-2	18	0.075	41	66	150	1.165×10^{-3}	2481.4	2.73	2130.0	908.9
BF-18-4	18	0.15	77	63	151	1.127×10^{-3}	4660.2	2.68	4135	1738.9
BF-18-8	18	0.3	103	66	151	1.181×10^{-3}	6233.8	2.79	5278.4	2234.3
BF-18-12	18	0.45	84	64	149	1.115×10^{-3}	5083.8	2.70	4559.5	1882.9
BF-18-16	18	0.6	20	64	151	1.145×10^{-3}	1210.4	2.69	1057.1	450.0

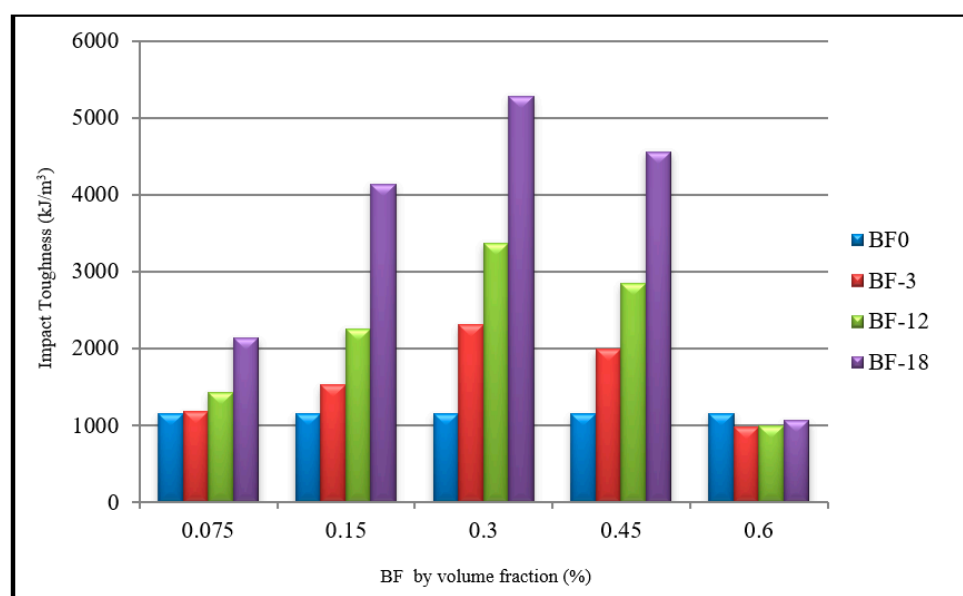


Figure 9. Average impact toughness results of BF specimens at a drop of 457 mm after 28 days.

At any given BF content, except 0.6%, increasing the fiber length increased the impact toughness. Using BF lengths of 3 mm, 12 mm, and 18 mm increased the impact toughness by 3%, 24%, and 86%, respectively, at 0.075% BF content; by 33%, 97%, and 261%, respectively, at 0.15% BF content; by 101%, 194%, and 361%, respectively, at 0.3% BF content; and by 73%, 149%, and 298%, respectively, at 0.45% BF content. The use of longer fibers demonstrated a stronger anchorage that enhanced the connectivity of the concrete matrix components, and hence resulted in relatively higher impact toughness.

Increasing the BF content to 0.6% decreased the impact toughness by 15%, 14%, and 8%, respectively, at 3 mm, 12 mm, and 18 mm length BF. At 0.6% BF content, the impact toughness decreased by 8–16% regardless of the BF length. The adverse effect of BF used at 0.6% content with any length was due to the BF balling and having lesser distribution within the concrete matrix, which caused multiple voids and resulted in easy crack propagation under impact loading.

Figure 10 shows the failure mode of some HPC specimens under impact loading. In BF-0 mix, the crack extended from the specimen center in the radial direction toward the specimen perimeter which exhibited brittle and sudden failure (single large crack). This was due to the low tensile strength and lack of bonding in the transition zone between the aggregate and cement matrix which obviously restricted the utilization of the HPC under dynamic loading as shown in Figure 10a. Similar results were obtained in the HPC mixes with different BF contents resulting in a slight change in failure patterns and the occurrence of a single crack as shown in Figure 10b,c.

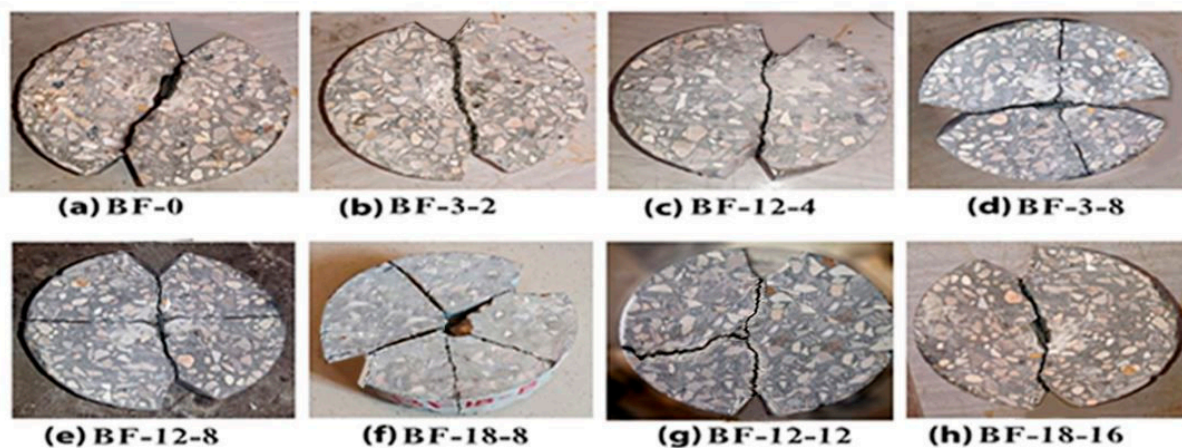


Figure 10. Fracture pattern of concrete with different fiber volume fractions under the drop-weight test.

Moreover, the addition of BF at 8 kg/m^3 to the concrete improves the high resistance and maximum displacement response, in addition to changing from a single crack to multiple cracks as shown in Figure 10d–f. In terms of Figure 10g, it is notable that there are two apparent cracks due to adding basalt fibers at 12 kg/m^3 . Clearly, such a formed shape is considered to have a recommended pattern because of the ability of basalt fibers to bridge apparent cracks often according to stress, which further enhances the ductility and effectively reduces the brittleness of the specimens. However, adding basalt fibers at 16 kg/m^3 leads to the failure crack pattern being changed from group cracks to a single crack. Owing to the basalt fiber that is balled and is not distributed well inside the concrete, this results in voids that reduce the strength of the concrete and the failure of crack patterns are similar to that of the plain concrete as shown in Figure 10h.

The results denote the ability of BF to bridge the cracks at higher strain levels in the specimens of high-performance concrete (HPC), resulting in a better ductility response. It can also be seen that the HPC specimens with an 8 kg/m^3 basalt fiber content exhibit higher superiority in ultimate resistance and deformation capacity. Significant stress redistribution is observed after the cracking of the HPC specimen with a chopped basalt fiber

content of 8 kg/m^3 , demonstrated by a deflection-hardening response. A ductile failure, under impact loading, is also observed in the fiber specimens.

Generally, the mixtures containing BF are essential especially in impact resistance strength in the case of comparison to the control mixture without BF (0%). All specimens containing BF are clearly influential in preventing separation through bridging the crack due to the increase in bond strength and coherence across the cement paste within the mixtures containing BF in addition to coarse aggregate. Such additions demonstrate the domains in which BF would be beneficial to high-performance concrete (HPC), which are the domains that are submitted to such impact loading. It is clear that BF has a clear effectiveness in a specimen's brittleness reduction; in addition, fibers improve the concrete's ability to absorb such kinetic energy.

3.4. Relationship between Impact Energy and Compressive Strength

The relationship between the impact energy and compressive strength of basalt-fiber-reinforced high-performance concrete at ultimate failure has been developed by regression analysis as shown in Figure 11. As the volume fraction of basalt fiber increased; both the compressive strength and the impact energy were increased. The correlative co-efficiency for all the specimens has been 0.667 at 457 mm height.

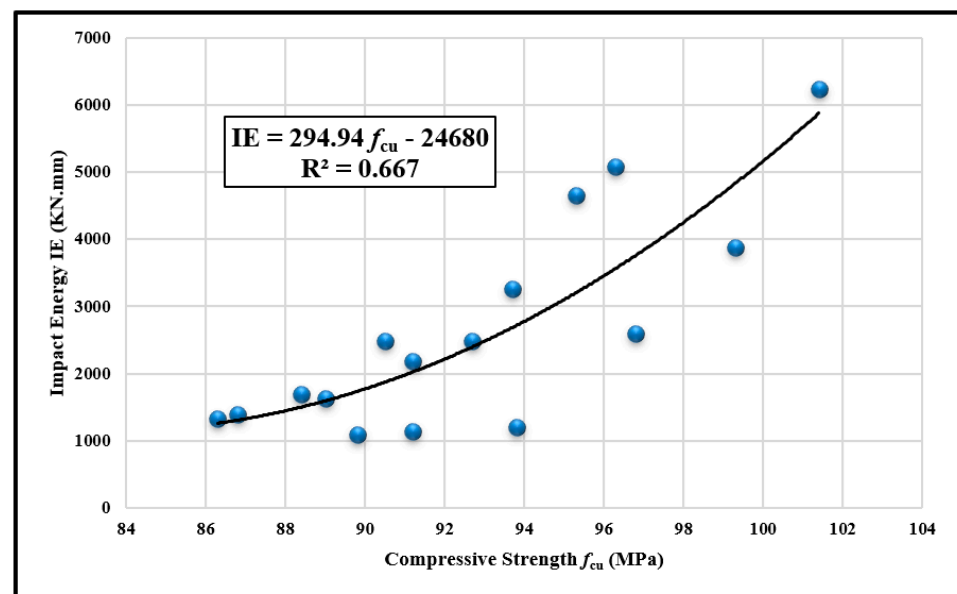


Figure 11. Relationship between impact energy and compressive strength.

It can be seen in Table 5 that the predicted value of impact energy is obtained from the regression equation. These predicate values are in good agreement with the experimental observations [39]. In the view of convenience and generality, the empirical relationship is accurate and preferable to evaluate the impact energy by using the compressive strength of basalt-fiber-reinforced concrete with carrying out the drop-weight test [40].

3.5. Microstructural Analysis

SEM analysis was carried out on concrete samples taken from some HPC mixes tested at 56 days in compression and shown in Figure 12. In the mix BF-0 that contains no basalt fibers, many components were observed, namely the following: calcium silicate hydrate (C-S-H); calcium hydroxide ($\text{Ca}(\text{OH})_2$); in addition to many pores and cracks that were found in the interfacial transition zone (ITZ). This led to a relatively low compressive strength compared with the other mixes as shown Figure 12a. In Figure 12b, the presence of BF in mix BF-18-8 resulted in a strength increase by bridging the cracks, and the basalt fibers appear to be well embedded and connected to the matrix.

Regarding Figure 12c, the BFs that are embedded also generate some cracks with random orientations which would decrease the strength but increase the deformability by debonding between the cement and aggregates. This is mainly due to the effectiveness of the basalt fiber in preventing the growth and scope of cracks within the concrete's structure, which gradually prevents the concrete's strength weakness to allow the concrete to preserve and retain some post-cracked strength and to resist any apparent deformations much more than the concrete without fiber [41,42]. For the BF-reinforced concrete, the BFs are embedded within the matrix, which fills the pore space so that less crystalline CH in addition to a much more C-S-H gel-like phase is produced. Thus, such a case leads to a higher strength and density than that of the plain concrete as shown in Figure 12d.

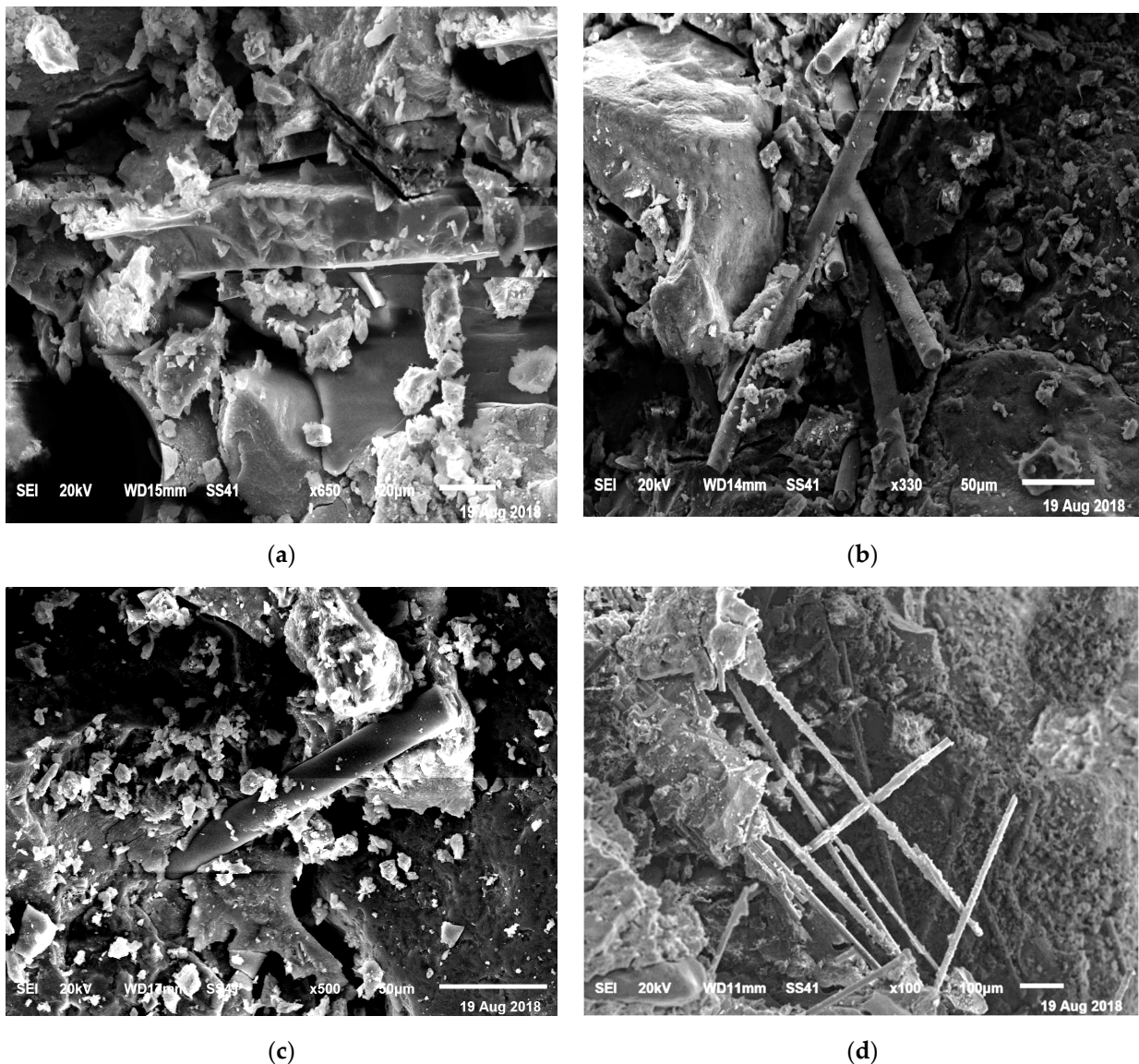


Figure 12. SEM images of mixes: (a) BF-0 at $\times 650$, (b) BF-18-8 at $\times 330$, (c) BF-18-8 at $\times 500$, and (d) BF-18-8 at $\times 100$.

4. Conclusions

This laboratory study examined the compressive strength and impact resistance of HPC with basalt fibers. The effect of basalt fibers at different volume fractions on the HPC was evaluated. Additionally, microstructures were investigated by scanning electronic microscopy SEM. Based on the study, the following conclusions can be drawn:

1. BF was added to the high-performance concrete with the aim of increasing both the ductility and the mechanical properties. The amount of BF influenced the workability of the final product.
2. Using chopped basalt fibers enhanced the compressive strength of the concrete. The optimum compressive strength value was obtained using a BF content of 8 kg/m³. When the volume fraction of basalt fiber was 8 kg/m³, the compressive strength was increased by 16.00%, 17.50%, and 14.45% at ages 2, 28, and 56 days, respectively, compared with that of HPC without fiber.
3. The empirical relationship between the impact energy and compressive strength, obtained from regression analysis, shows that the predictable values are in a good agreement and integration with the empirical data.
4. Based on the experimental results, the addition of BF increased the number of blows that the high-performance concrete was subjected to at ultimate failure compared with HPC without fiber. Moreover, the results indicated this addition of BF significantly influenced the impact toughness of the concrete when subjected to impact loading. In the case of impact loading, the impact toughness significantly increased with a dosage of 8 kg/m³ of BF compared with reference concrete. Therefore, the failure mechanism showed less brittleness throughout, changing from a diagonal to a radial failure pattern.
5. The SEM observations of the concrete showed that the BFs which accumulated in pores and on the surface of the attached mortar could both strengthen the concrete and improve the microstructure of the interfacial transition zone (ITZ), which further enhanced the bonding strength and ductility of the concrete.
6. It is recommended for future studies to further develop and verify the relationship between the concrete impact resistance and compressive strength using more experimental measurements.

Author Contributions: Conceptualization, A.M.T. and K.A.H.; formal analysis, K.A.H.; investigation, K.A.H. and O.Y.; methodology, A.M.T. and O.Y.; project administration, O.Y.; resources, A.M.T.; software, K.A.H.; supervision, O.Y.; validation, K.A.H.; writing—original draft, K.A.H. and O.Y.; writing—review & editing, A.M.T. and O.Y. All authors have read and agreed to the published version of the manuscript.

Funding: This research received no external funding.

Institutional Review Board Statement: Not applicable.

Informed Consent Statement: Not applicable.

Data Availability Statement: No new data were created.

Conflicts of Interest: The authors declare no conflict of interest.

References

1. Zhou, A.; Qin, R.; Feo, L.; Penna, R.; Lau, D. Investigation on interfacial defect criticality of FRP-bonded concrete beams. *Compos. B Eng.* **2017**, *80–90*, 113. [[CrossRef](#)]
2. Abbass, W.; Khan, M.I.; Mourad, S. Evaluation of mechanical properties of steel fiber reinforced concrete with different strengths of concrete. *Construct. Build. Mater.* **2018**, *168*, 556–569. [[CrossRef](#)]
3. Lee, J.; Cho, B.; Choi, E. Flexural capacity of fiber reinforced concrete with a consideration of concrete strength and fiber content. *Construct. Build. Mater.* **2017**, *138*, 222–231. [[CrossRef](#)]
4. Branston, J.; Das, S.; Kenno, S.Y.; Taylor, C. Mechanical Behavior of Basalt Fiber Reinforced Concrete. *Constr. Build. Mater.* **2016**, *124*, 878–886. [[CrossRef](#)]
5. Olalusi, O.B.; Awoyera, P. Shear capacity prediction of slender reinforced concrete structures with steel fibers using machine learning. *Eng. Struct.* **2021**, *227*, 111470. [[CrossRef](#)]
6. Okeh, C.A.O.; Begg, D.W.; Barnett, S.J.; Nanos, N. Behaviour of hybrid steel fiber reinforced self-compacting concrete using innovative hooked-end steel fibers under tensile stress. *Constr. Build. Mater.* **2019**, *202*, 753–761. [[CrossRef](#)]
7. Villar, V.P.; Medina, N.F.; Alonso, M.M.; Diez, S.G.; Puertas, F. Assessment of parameters governing the steel fiber alignment in fresh cement-based composites. *Constr. Build. Mater.* **2019**, *207*, 548–562. [[CrossRef](#)]

8. Luo, D.; Khater, A.; Yue, Y.; Abdel Salam, M.; Zhang, Z.; Li, Y.; Li, J.; Iseley, D.T. The performance of asphalt mixtures modified with lignin fiber and glass fiber: A review. *Constr. Build. Mater.* **2019**, *209*, 377–387. [[CrossRef](#)]
9. Schneider, K.; Michel, A.; Liebscher, M.; Terreri, L.; Hempel, S.; Mechtcherine, V. Mineral-impregnated carbon fiber reinforcement for high temperature resistance of thin-walled concrete structures. *Cem. Concr. Compos.* **2019**, *97*, 68–77. [[CrossRef](#)]
10. Chen, X.; Kou, S.; Xing, F. Mechanical and durable properties of chopped basalt fiber reinforced recycled aggregate concrete and the mathematical modeling. *Constr. Build. Mater.* **2021**, *298*, 123901. [[CrossRef](#)]
11. Youssf, O.; ElGawady, M.A.; Mills, J.E.; Ma, X. Finite element modelling and dilation of FRP-confined concrete columns. *Eng. Struct.* **2014**, *79*, 70–85. [[CrossRef](#)]
12. Youssf, O.; Hassanli, R.; Mills, J.E. Retrofitting square columns using FRP-confined crumb rubber concrete to improve confinement efficiency. *Constr. Build. Mater.* **2017**, *153*, 146–156. [[CrossRef](#)]
13. Elchalakani, M. High strength rubberized concrete containing silica fume for the construction of sustainable road side barriers. *Structures* **2015**, *1*, 20–38. [[CrossRef](#)]
14. Youssf, O.; Hassanli, R.; Mills, J.E. Mechanical performance of FRP-confined and unconfined crumb rubber concrete containing high rubber content. *J. Build. Eng.* **2017**, *11*, 115–126. [[CrossRef](#)]
15. Fiore, V.; Scalici, T.; Di Bella, G.; Valenza, A. A review on basalt fiber and its composites. *Compos. B Eng.* **2015**, *74*, 74–94. [[CrossRef](#)]
16. Sadrmomtazi, A.; Tahmouresi, B.; Saradar, A. Effects of silica fume on mechanical strength and microstructure of basalt fiber reinforced cementitious composites (BFRCC). *Constr. Build. Mater.* **2018**, *162*, 321–333. [[CrossRef](#)]
17. Ralegaonkar, R.; Gavali, H.; Aswath, P.; Abolmaali, S. Application of chopped basalt fibers in reinforced mortar: A review. *Constr. Build. Mater.* **2018**, *164*, 589–602. [[CrossRef](#)]
18. Alaskar, A.; Albidah, A.; Alqarni, A.; Alyousef, R.; Mohammadhosseini, H. Performance evaluation of high-strength concrete reinforced with basalt fibers exposed to elevated temperatures. *J. Build. Eng.* **2021**, *35*, 102108. [[CrossRef](#)]
19. Ozen, M.; Algin, Z. The properties of chopped basalt fiber reinforced self-compacting concrete. *Constr. Build. Mater.* **2018**, *186*, 678–685.
20. Niu, D.; Su, L.; Luo, Y.; Huang, D.; Luo, D. Experimental study on mechanical properties and durability of basalt fiber reinforced coral aggregate concrete. *Constr. Build. Mater.* **2020**, *237*, 117628. [[CrossRef](#)]
21. Jiang, C.; Fan, K.; Wu, F.; Chen, D. Experimental Study on Mechanical Properties and Microstructure of Chopped Basalt Fiber Reinforced Concrete. *Mater. Design.* **2014**, *58*, 187–193. [[CrossRef](#)]
22. Adesina, A. Performance of cementitious composites reinforced with chopped basalt fibers—An overview. *Constr. Build. Mater.* **2021**, *266*, 120970. [[CrossRef](#)]
23. Elshafie, S.; Whittleston, G. A Review of the Effect of Basalt Fiber Lengths and Proportions on the Mechanical Properties of Concrete. *Int. J. Res. Eng. Technol.* **2015**, *4*, 458–465.
24. Wang, D.; Ju, Y.; Shen, H.; Xu, L. Mechanical Properties of High-Performance Concrete Reinforced with Basalt Fiber and Polypropylene Fiber. *Constr. Build. Mater.* **2019**, *197*, 464–473. [[CrossRef](#)]
25. Irine, F. Strength Aspects of Basalt Fiber Reinforced Concrete. *Int. J. Innov. Res. Advert. Eng.* **2014**, *1*, 192–198.
26. Kathuda, H.; Shatarat, N. Improving the Mechanical Properties of Recycled Concrete Aggregate Using Chopped Basalt Fibers and Acid Treatment. *Constr. Build. Mater.* **2017**, *140*, 328–335. [[CrossRef](#)]
27. Afroughsabet, V.; Biolzi, L.; Ozbakkaloglu, T. High-performance fiber-reinforced concrete: A review. *J. Mater. Sci.* **2016**, *51*, 6517–6551. [[CrossRef](#)]
28. Mehta, P.K.; Aitcin, P.C. *Cementitious Concrete and Aggregates*; American Society for Testing Materials: Philadelphia, PA, USA, 1990; Volume 12, pp. 70–78.
29. Ahmed, S.F.U.; Maalej, M. Tensile strain hardening behaviour of hybrid steel polyethylene fiber reinforced cementitious composites. *Constr. Build. Mater.* **2009**, *23*, 96–106. [[CrossRef](#)]
30. Li, W.; Xu, J. Mechanical Properties of Basalt Fiber Reinforced Geo-Polymeric Concrete under Impact Loading. *Mater. Sci. Eng. A* **2009**, *505*, 178–186. [[CrossRef](#)]
31. *ES 4756-1/*; Cement-Part 1: Composition, Specifications and Conformity Criteria for Common Cements. Egyptian Organization for Standardization and Quality: Cairo, Egypt, 2013.
32. *Egyptian Standard, ES: 1109/*; Aggregates for Concrete. Egyptian Organization for Standardization and Quality: Cairo, Egypt, 2008.
33. *ASTM C494*; Standard Specification of Chemical Admixtures for Concrete. American Society for Testing and Materials Standard Practice C494: Philadelphia, PA, USA, 2004.
34. *Egyptian Standard, ES: 2421/*; Cement-Physical and Mechanical Testing. Egyptian Organization for Standardization and Quality Control: Cairo, Egypt, 2009.
35. *ACI Committee 544.2R-89*; Measurement of Properties of Fiber Reinforced Concrete. ACI: West Conshohocken, PA, USA, 1999.
36. Badr, A.; Ashour, A.F. Modified ACI Drop-weight Impact Test for Concrete. *ACI Mater. J.* **2005**, *102*, 249–255.
37. Siddique, S.; Shrivastava, S.; Chaudhary, S.; Gupta, T. Strength and Impact Resistance Properties of Concrete Containing Fine Bone China Ceramic Aggregate. *Constr. Build. Mater.* **2018**, *169*, 289–298. Available online: <https://doi.org.ezproxy.library.unlv.edu/10.1016/j.conbuildmat.2018.02.213> (accessed on 15 September 2020). [[CrossRef](#)]
38. Abdel Aleem, B.H.; Ismail, M.K.; Hassan, A.A.A. The Combined Effect of Crumb Rubber and Synthetic Fibers on Impact Resistance of Self-consolidating Concrete. *Constr. Build. Mater.* **2018**, *162*, 816–829. Available online: <https://doi.org.ezproxy.library.unlv.edu/10.1016/j.conbuildmat.2017.12.077> (accessed on 3 November 2020). [[CrossRef](#)]

39. Murali, G.; Santhi, A.S.; Ganesh, G.M. Empirical Relationship between the Impact Energy and Compressive Strength for Fiber Reinforced Concrete. *J. Sci. Ind. Res.* **2014**, *73*, 469–473.
40. Myers, J.J.; Tinsley, M. Impact resistance of blast mitigation material using modified ACI drop-weight impact test. *ACI Mater. J.* **2013**, *110*, 339–348.
41. Niaki, M.H.; Fereidoon, A.; Ahangari, M.G. Experimental study on the mechanical and thermal properties of basalt fiber and nano clay reinforced polymer concrete. *Compos. Struct.* **2018**, *191*, 231–238. [[CrossRef](#)]
42. Dong, J.F.; Wang, Q.Y.; Guan, Z.W. Material Properties of Basalt Fiber Reinforced Concrete Made with Recycled Earthquake Waste. *Constr. Build. Mater.* **2017**, *130*, 241–251. [[CrossRef](#)]

Disclaimer/Publisher’s Note: The statements, opinions and data contained in all publications are solely those of the individual author(s) and contributor(s) and not of MDPI and/or the editor(s). MDPI and/or the editor(s) disclaim responsibility for any injury to people or property resulting from any ideas, methods, instructions or products referred to in the content.